Electron scattering from a deeply bound nucleon on the light-front

Frank Vera and Misak M. Sargsian
Department of Physics, Florida International University, Miami, Florida 33199, USA

(Received 1 June 2018; revised manuscript received 9 August 2018; published 27 September 2018)

We calculate the cross section of the electron scattering from a bound nucleon within light-front approximation. The advantage of this approximation is the possibility of systematic account for the off-shell effects, which become essential in high-energy electronuclear processes aimed at probing the nuclear structure at small distances. We derive a new dynamical parameter, which allows us to control the extent of the off-shellness of electron–bound-nucleon electromagnetic current for different regions of momentum transfer and initial light-cone momenta of the bound nucleon. The derived cross section is compared with the results of other approaches in treating the off-shell effects in electron-nucleon scattering.

DOI: 10.1103/PhysRevC.98.035202

I. INTRODUCTION

High-energy electronuclear processes ranging from inclusive $A(e,e')X$ to the double $A(e,e'N_f)X$ and triple $A(e,e'N_f,N_r)X$ coincidence reactions, in which e' is the scattered electron, N_f and N_r are struck and recoil nucleons are the main processes used to probe the short-range structure of nuclei. During the last two decades a multitude of dedicated experiments have been performed that significantly advanced our understanding of the dynamics of short-range nucleon correlations in nuclei (for recent reviews on this subject see Refs. [1–6]). All of these experiments were performed at quasielastic kinematics in which electrons are scattered off the deeply bound nucleon producing a struck nucleon (N_f) in the final state. Here, deeply bound nucleon is defined as an off-shell nucleon with momentum $p_i \gtrsim 300$ MeV/c and removal energy, $E_m \sim \sqrt{m_N^2+p_i^2}-m_N$. The observed experimental signatures were in agreement with the expectations that deeply bound nucleons emerge from short-range nucleon-nucleon correlations (SRCs). These signatures included the onset of scaling for the inclusive $A(e,e')X$ cross section ratios of nucleus A to the deuteron or ^{3}He [7–10], strong angular correlation between momenta of struck N_f and recoil N_r nucleons [11,12] as well as significant dominance of the pn correlations [13–16] in the domain of $2N$ SRCs.

The next stage of SRC studies requires the exploration of quantitative properties of the nuclear structure describing nucleons in the SRC. This research can be both experimental, performing extraction of nuclear spectral and decay functions in the region of high momentum and removal energy of the struck nucleon, or theoretical, by modeling these structure functions (see, e.g., Ref. [17]) and predicting electroproduction cross sections in large missing momentum and removal energy kinematics. One of the outstanding problems in such research is the understanding of the reaction mechanism and final-state interaction (FSI) effects associated with the electron scattering from a deeply bound nucleon in the nucleus.

During the last two decades significant efforts have been made in the calculation of FSI effects in high Q^2 electronuclear processes (see, e.g., Refs. [18–27]). One of the approaches, referred to as generalized eikonal approximation [18,25], self-consistently treated the relativistic effects associated with the large momentum of the bound nucleon involved in the reaction, as such these approach provided a theoretical framework for calculating FSI effects relevant to studies of the nuclear structure at short distances.

However, not much theoretical attention is given currently to the studies of the reaction mechanism of elastic scattering from the high-momentum bound nucleon in the nucleus. The problem of the proper description of electromagnetic scattering from deeply bound nucleon in the nucleus was realized in the 1980's with the advent of the intermediate energy $A(e,e'N_f)$ experiments at SACLAY [28,29] and NIKHEF [30]. The first approaches in describing electron–deeply-bound-nucleon scattering were based on different methods of interpreting the spinor of the bound (off-shell) nucleon. In one of the earlier models [31] the on-shell nucleon spinors were used with the mass estimated as $m_N^{*2}=E^2-p^2$. Currently the most popular model is that of de Forest [32] in which different expressions for the $eN_{\rm bound}$ cross sections are obtained based on the different assumptions for effective $\gamma^* N_{\rm bound}$ vertices with on-shell spinors used for the bound nucleon. No preference is given to any of the considered eight expressions of the $eN_{\rm bound}$ cross section and as such these approximations allowed us to check uncertainty due to the binding effects rather than calculating their actual values. Such an approach was characteristic to the intermediate energy (few hundred MeV of incoming beam energy) scattering processes in which no small parameters existed in treating the strong binding effects in nucleon electromagnetic current.

The situation has recently changed with the emergence of high-energy and momentum transfer eA experiments (see, e.g., Refs. [1,3,5]) in which deeply bound nucleons in the nucleus are probed with high Q^2 virtual photons producing final nucleons with momenta above few GeV/c region. The high-energy nature of the scattering process allows for important simplifications in describing the scattering process similar to those in hadronic physics. One of the main

characteristics of high-energy scattering is that the process evolves along the light-front (see, e.g., Refs. [33–37]), which makes the light cone the most natural reference frame to describe the reaction. The important advantage of such description is the suppression of the negative energy contribution in the propagator of bound nucleon as well as the possibility of identifying the good component of electromagnetic current for which the off-shell effects are minimal. There have been several extensive studies of nuclear dynamics on light-front (see, e.g., Refs. [36,38–40]) with the main emphasis given to the description of the nuclear structure in relativistic kinematics.

In the current work we focus on light-front treatment of the electron–bound-nucleon interaction. Based on the effective light-front perturbation theory, we calculate the cross section of electron–bound-nucleon scattering by explicit separation of the propagating (prop) and instantaneous (inst) contributions. Within light-front approach we introduced a new, parameter η, which allows us to quantify the off-shellness of the $\gamma^* N_{\rm bound}$ scattering universally for any kinematical situation. The derived expressions are compared with the off-shell cross sections, which are currently being used in the description of electronuclear reactions. We also present numerical analysis of our calculations where we identify kinematics in which off-shell effects can be suppressed or isolated for dedicated investigation of bound nucleon properties. The numerical analysis allows us to conclude that by restricting the new off-shell parameter $\eta < 0.1$ one can confine the off-shell effects below 5% for any realistic values of bound nucleon momenta at different Q^2 of electroproduction reaction.

In Sec. II we set up the calculations isolating the electromagnetic hadronic tensor for exclusive $d(e,e'N)N$ scattering within plane wave impulse approximation (PWIA). We discuss here the main problems associated with probing deeply bound nucleons, namely the increased role of the vacuum fluctuations and identification of the nuclear wave function for a bound nucleon. Section III presents the calculation of the PWIA diagram within effective light-front perturbation theory and identification of the propagating and instantaneous components of the bound nucleon electromagnetic current. We also introduce the boost invariant off-shell parameter that naturally quantifies the off-shell effects in the light-front approach. In Sec. IV we present the results in the form of the electron–bound-nucleon cross section σ_{eN}, which is compared with the predictions of other approaches in Sec. V. Section VI presents the summary of the results and outlook on possible extension beyond PWIA approximation. In Appendix A we give the diagrammatic rules of effective light-front perturbation theory. The details of derivation of the bound nucleon structure functions are presented in Appendix B.

II. SETTING UP THE CALCULATION

The simplest case of electroproduction process involving electron scattering from a bound nucleon is the reaction:

$$e + d \to e' + N_f + N_r, \tag{1}$$

in which one of the nucleons is knocked out (N_f) by the virtual photon and the other is treated as a recoil (N_r).

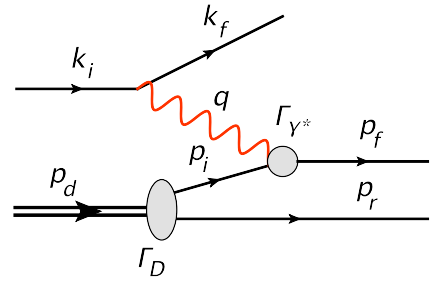

FIG. 1. Exclusive electrodisintegration of the deuteron in plane wave impulse approximation.

Deuteron represents as testing ground for development of many relativistic approaches in description of electronuclear processes (see, e.g., Refs. [38,41–43]), which in principle can be generalized for medium to heavy nuclei.

For our purpose of defining the cross section of electron–bound-nucleon scattering we consider the single photon exchange case of the above reaction within covariant plane wave impulse approximation (PWIA) corresponding to the diagram of Fig. 1.

Here, within PWIA the off-shellness of the bound nucleon is completely defined by the four-momentum of the deuteron, p_d and spectator nucleon p_r: $p_i = p_D - p_r$. The one-photon exchange approximation allows us to factorize electron and hadronic parts of the interaction in the invariant Feynman amplitude presented as follows:

$$\mathcal{M} = \langle \lambda_f | j_e^\nu | \lambda_i \rangle \frac{e^2 g_{\nu\mu}}{q^2} \langle s_f, s_r | A_0^\mu | s_d \rangle, \tag{2}$$

where q^2 is the virtual photon's momentum squared. Here the leptonic current j_e^ν is defined as:

$$\langle \lambda_f | j_e^\nu | \lambda_i \rangle = \bar{u}(k_f, \lambda_f) \gamma^\nu u(k_i, \lambda_i), \tag{3}$$

where $\langle s_f, s_r | A_0^\mu | s_d \rangle$ represents the invariant amplitude of $\gamma^* d \to NN$ scattering,

Using Eq. (2) for the differential cross section of reaction (1) one obtains:

$$\frac{d\sigma}{d^3k_f/\epsilon_f d^3p_f/E_f} = \frac{1}{4\sqrt{(p_d\cdot k_i)^2}} \frac{e^4}{q^4} L^{\mu\nu} H_{\mu\nu} \frac{\delta\left[(q+p_d-p_f)^2 - m_N^2\right]}{4(2\pi)^5}. \tag{4}$$

where terms proportional to electron's mass squared (m_e^2) are neglected. Here the leptonic tensor is defined as:

$$L^{\mu\nu} = \frac{1}{2} \sum_{\lambda_1\lambda_2} (\bar{u}(k_f, \lambda_f)\gamma^\nu u(k_i, \lambda_i))^\dagger \bar{u}(k_f, \lambda_f)\gamma^\mu u(k_i, \lambda_i) \tag{5}$$

whereas the nuclear electromagnetic tensor is expressed through the scattering amplitude A_0^μ as follows:

$$H^{\mu\nu} = \frac{1}{3} \sum_{s_d s_r s_f} \langle s_d | A_0^{\mu\dagger} | s_f, s_r \rangle \langle s_f, s_r | A_0^\nu | s_d \rangle. \tag{6}$$

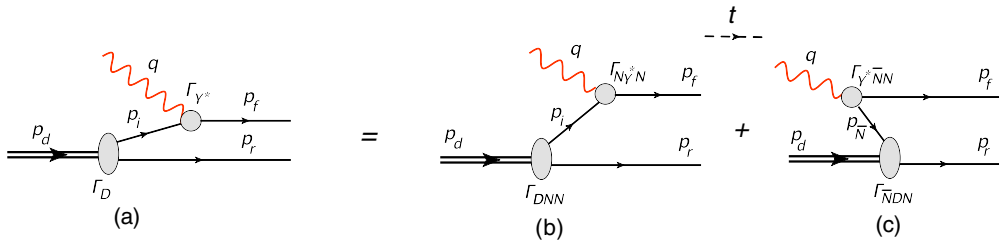

FIG. 2. Representation of the covariant scattering amplitude (a) as a sum of two time-ordered diagrams. (b) Virtual photon scattering from the bound nucleon. (c) Production of the $\bar{N}N$ pair by the virtual photon with subsequent absorption of the antinucleon by the deuteron.

If one introduces $\Gamma^{\mu}_{\gamma^*}$ and Γ_D invariant vertices (Fig. 1) then within PWIA the amplitude A^{μ}_0 can be presented in the form:

$$\langle s_f, s_r | A^{\mu}_0 | s_d \rangle = -\bar{u}(p_f, s_f)\Gamma^{\mu}_{\gamma^*}\frac{\not{p}_i + m_N}{p_i^2 - m_N^2}\cdot \bar{u}(p_r, s_r)\Gamma_D \cdot \chi^{s_d}, \quad (7)$$

where χ^{s_d} is the spin wave function of the deuteron.

As it follows from the above equation A^{μ}_0 contains neither the electron–bound-nucleon scattering nor the nuclear wave function in the explicit form. The eN_{bound} scattering and the nuclear wave function appears only when one considers the amplitude of Fig. 1 in a time-ordered perturbation theory in which case the invariant Feynman diagram splits into two time orderings as presented in Fig. 2.

Here, Fig. 2(b) represents a scenario in which the virtual photon interacts with the preexisting bound nucleon in the deuteron with Γ_{DNN} representing the vertex of $D \to NN$ transition and $\Gamma_{N\gamma^*N}$ the $\gamma^*N \to N$ electromagnetic interaction. This contribution corresponds to the noncovariant PWIA in which case the eA cross section is expressed through the product of eN cross section and noncovariant nuclear spectral function. Figure 2(c), however, represents a very different scenario, in this case the virtual photon produces an intermediate $\bar{N}N$ state at the $\Gamma_{\gamma^*\bar{N}N}$ vertex with subsequent absorption of the antinucleon, $\bar{N}$ in the deuteron at the $\Gamma_{\bar{N}DN}$ vertex. The latter is not related to the γ^*N scattering and the nucleon wave function in the deuteron. Figure 2(c) is commonly referred to as a Z graph and is a purely relativistic effect. As a result in the nonrelativistic limit one deals with the diagram of Fig. 2(b) only, which allows us to express the covariant scattering amplitude through the nonrelativistic nuclear wave function and γ^*N_{bound} scattering amplitude. However, the situation becomes complicated when one is interested in the bound nucleon momentum $p_i \sim M_N$, which can be probed at momentum transfer $q \gg M_N$. In this case the Z-graph contribution [Fig. 2(c)] becomes comparable with the one in Fig. 2(b) preventing the straightforward introduction of the nuclear wave function. Thus conventional noncovariant PWIA is inapplicable for the description of electron scattering from deeply bound (relativistic) nucleons in the nucleus.

This situation is reminiscent of the QCD processes in probing partonic structure of hadrons in which case due to the relativistic nature of partons, vacuum diagrams can not be neglected in the time-ordered perturbation theory defined in the laboratory frame of the hadron [33]. The solution in this case is to consider the scattering process in the infinite momentum frame (or on the light-front), which allows us to suppress the Z graphs and consider only the diagrams similar to Fig. 2(b) for which one can introduce the wave function of the constituents.

Our approach in probing deeply bound nucleon is similar to that of the partonic model, in which we consider the reaction (1) on the light-front allowing us to exclude the contribution of the vacuum diagrams [Fig. 2(c)] and introduce a light-front nuclear wave function.

III. DERIVATION WITHIN EFFECTIVE LIGHT-FRONT PERTURBATION THEORY

A. Scattering amplitude in PWIA

We consider now the reaction (1) on the light-front, where the light-cone time is defined as $\tau \equiv t + z$. To calculate the PWIA amplitude of the reaction (1) we apply effective light-front perturbation theory (LFPT) in the τ-time-ordered representation of the scattering amplitude A^{μ}_0. In such approach the scattering amplitude (7) is expressed as a sum of the noncovariant diagrams presented in Fig. 3. Here in addition to the two τ orderings analogous to the time ordering of Fig. 2 one has an additional contribution of Fig. 3(c) corresponding to the instantaneous interaction due to the spinor nature of the bound nucleon.

To proceed with the calculations we choose a reference frame with z axis antiparallel to the transferred momentum, $\hat{z} \| -\mathbf{q}$, such that the deuteron is aligned along $\hat{z}$.

The calculations are performed in the light-cone (LC) reference frame in which case where the four-momenta are defined as (p^+, p^-, p_x, p_y), where $p^{\pm} = E \pm p_z$ with p^+ representing the light-cone longitudinal momentum. We employ the γ-matrix algebra using the following light-cone definitions:

$$\gamma^{\mu} = (\gamma^+, \gamma^-, \gamma_1, \gamma_2), \quad \text{where} \quad \gamma^{\pm} = \gamma_0 \pm \gamma_3. \quad (8)$$

The scalar products and other properties of four-vectors as well as γ matrices on the light-front are given in Appendix A.

We also define the light-cone momentum fractions, which are Lorentz invariant quantities with respect to boosts along

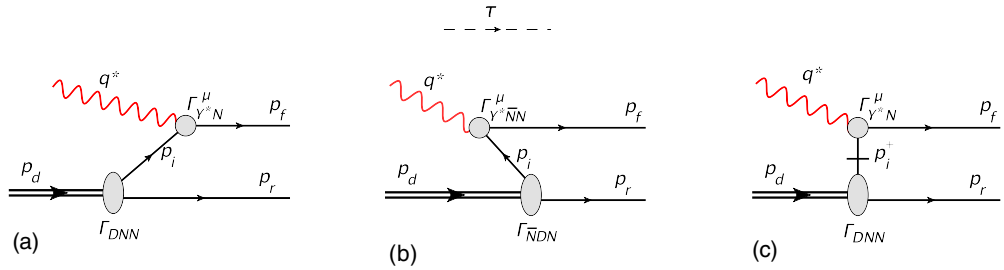

FIG. 3. Representation of the covariant scattering amplitude as a sum of two light-cone (τ)-time -ordered diagrams as well as instantaneous interaction. (a) Virtual photon scattering from the bound nucleon. (b) Production of the $\bar{N}N$ pair by the virtual photon with subsequent absorption of the antinucleon by the deuteron. (c) Instantaneous interaction of virtual photon with the bound nucleon.

the z direction:

$$\alpha_r = \frac{2p_r^+}{p_d^+}, \quad \alpha_q = \frac{2q^+}{p_d^+},$$
$$\alpha_f = \frac{2p_f^+}{p_d^+}, \quad \alpha_N = \alpha_f - \alpha_q = 2 - \alpha_r. \tag{9}$$

Here α_r, α_q, and α_f correspond to the fraction of LC "+" component of the deuteron momentum carried by the recoil nucleon, virtual photon, and final knock-out nucleon, respectively. The light-cone momentum fraction of the bound nucleon α_N is defined through the energy-momentum conservation.

We proceed with the calculation of the scattering amplitude corresponding to the diagrams of Fig. 3 by applying the light-front perturbation rules [34,35] in an effective theory in which one identifies effective vertices for nuclear transition and electron–bound-nucleon scattering (see Appendix A). At each vertices the transverse, $p_\perp$ and plus, p^+ components of momenta are conserved. Because of the latter and the chosen reference frame in which $q^+ = q_0 - |\mathbf{q}| < 0$ the diagram of the Fig. 3(b) will not contribute since the production of $\bar{N}N$ pair, which requires $q^+ > 0$ is kinematically forbidden.

The remaining diagrams represent the amplitudes in which the virtual photon knocks out a bound nucleon, which propagates from the $d \to NN$ transition vertex to the $\gamma^* N$ interaction point, $A^\mu_{\rm prop}$ [Fig. 3(a)], and the instantaneous amplitude, $A^\mu_{\rm inst}$ [Fig. 3(c)] in which $d \to NN$ transition and $\gamma^* N$ interaction take place at the same light-cone time τ. In both diagrams the nucleus exposes its constituents and the scattering takes place off the bound nucleon, which allows us to introduce the light-front nuclear wave function and the amplitude of $\gamma^* N_{\rm bound}$ scattering.

We now apply the light-front diagrammatic rules [35] (summarized in Appendix A), which yields for the propagating part of the scattering amplitude [Fig. 3(a)]:

$$\langle s_f, s_r | A^\mu_{\rm prop} | s_d \rangle = -\bar{u}(p_f, s_f)\Gamma^\mu_{\gamma^* N} \frac{1}{p_i^+} \frac{(\not{p}_i + m_N)_{\rm on}}{(p_d^- - p_r^- - p_{i,\rm on}^-)} \times \bar{u}(p_r, s_r)\Gamma_{DNN}\chi^{s_d}, \tag{10}$$

where p_d^-, p_r^-, and $p_{i,\rm on}^-$ are defined from the on-energy shell condition: $p^- = \frac{m_j^2 + p_{\perp,j}^2}{p_j^+}$ with $j = d, r, (i, \rm on)$. The "on" subscript in $(\not{p}_i + m_N)_{\rm on}$ indicates that all the components of the bound nucleon light-cone momenta are taken on-energy shell.

For the instantaneous diagram of Fig. 3(c) applying the rules of Appendix A one obtains:

$$\langle s_f, s_r | A^\mu_{\rm inst} | s_d \rangle = -\bar{u}(p_f, s_f)\Gamma^\mu_{\gamma^* N} \frac{1}{p_i^+} \left(\frac{1}{2}\gamma^+\right) \bar{u}(p_r, s_r)\Gamma_{DNN}\chi^{s_d}. \tag{11}$$

Note that in both expressions (10) and (11) one has the same nuclear, Γ_{DNN} and electromagnetic, $\Gamma_{\gamma^* N}$ vertices.

For further elaborations, we introduce the off-energy shell "−" component of the bound nucleon $p_i^- = p_d^- - p_r^-$, and using the definition: $p_j^- = \frac{m_j^2 + p_{j,\perp}^2}{p_j^+}$ for the on-energy-shell "−" component for $j = d, r$ as well as Eq. (9) one obtains:

$$\frac{1}{p_d^- - p_r^- - p_{i,\rm on}^-} = \frac{1}{p_i^- - p_{i,\rm on}^-} = \frac{p_d^+}{M_d^2 - 4\frac{(m_N^2 + p_\perp^2)}{\alpha(2-\alpha)}}. \tag{12}$$

Using the above relation as well as the sum rule relation for on-shell spinors:

$$(\not{p}_i + m_N)_{\rm on} = \sum_{s_i} [u(p_i, s_i)\bar{u}(p_i, s_i)]_{\rm on}, \tag{13}$$

for the sum of the two amplitudes in Eqs. (10) and (11) one obtains:

$$A^\mu = A^\mu_{\rm prop} + A^\mu_{\rm inst} = -\bar{u}(p_f, s_f)\Gamma^\mu_{\gamma^* N} \frac{\sum_{s_i} u(p_i, s_i)\bar{u}(p_i, s_i)}{\frac{\alpha}{2}\left(M_d^2 - 4\frac{m_N^2 + \mathbf{p}_T^2}{\alpha(2-\alpha)}\right)} \times \bar{u}(p_r, s_r)\Gamma_{DNN}\chi^{s_d} \tag{14}$$

$$-\bar{u}(p_f, s_f)\Gamma^\mu_{\gamma^* N} \frac{\frac{1}{2}\gamma^+(p_i^- - p_{i,\rm on}^-)}{\frac{\alpha}{2}\left(M_d^2 - 4\frac{m_N^2 + \mathbf{p}_T^2}{\alpha(2-\alpha)}\right)} \bar{u}(p_r, s_r)\Gamma_{DNN}\chi^{s_d}. \tag{15}$$

Within PWIA we can factorize the above expression in the form of a product of electromagnetic current and the

light-front nuclear wave function. For this we introduce the light-front wave functions in the form [17,36]:

$$\psi_{\rm LF}^{s_i s_r s_d}(\alpha, \mathbf{p_T}) = -\frac{\bar{u}(p_i, s_i)\bar{u}(p_r, s_r)\Gamma_{DNN}\chi^{s_d}}{\frac{1}{2}\left(M_d^2 - 4\frac{m_N^2+\mathbf{p_T}^2}{\alpha(2-\alpha)}\right)}\frac{1}{\sqrt{2(2\pi)^3}}. \tag{16}$$

From the above definition one also obtains:

$$\frac{1}{\frac{\alpha}{2}\left(M_d^2 - 4\frac{m_N^2+\mathbf{p_T}^2}{\alpha(2-\alpha)}\right)}\bar{u}(p_r, s_r)\Gamma_{DNN}\ \chi^{s_d} = -\sum_{s_i}\frac{u(p_i, s_i)}{2m_N}\frac{\psi_{\rm LF}^{s_i s_r s_d}(\alpha, \mathbf{p_T})}{\alpha}\sqrt{2(2\pi)^3}. \tag{17}$$

Using now the above Eqs. (16) and (17) in $A^\mu_{\rm prop}$ and $A^\mu_{\rm inst}$, respectively, the Eq. (15) can be presented in the form:

$$A^\mu = A^\mu_{\rm prop} + A^\mu_{\rm inst} = \sum_{s_i} J^\mu_N(p_f s_f, p_i s_i)\frac{\psi_{\rm LF}^{s_i s_r s_d}(\alpha, \mathbf{p_T})}{\alpha}\sqrt{2(2\pi)^3}, \tag{18}$$

where we introduced the electromagnetic current of the bound nucleon as follows:

$$J^\mu_N(p_f s_f, p_i s_i) = \bar{u}(p_f s_f)\Gamma^\mu_{\gamma^* N}u(p_i s_i) + \bar{u}(p_f s_f)\Gamma^\mu_{\gamma^* N}\frac{\gamma^+(p_i^- - p_{i\,\rm on}^-)}{4m_N}u(p_i s_i). \tag{19}$$

Here, the Dirac spinor of the initial nucleon $u(p_i, s_i)$ is defined for the on-shell momentum, $p_{i,\rm on} = (p_{i,\rm on}^-, p_i^+, p_i^\perp)$. As one observes from Eq. (18) the price one pays for eliminating the vacuum diagram [Fig. 3(b)] on the light-front is the need to calculate electron–bound-nucleon scattering and the nuclear wave function in the light-front reference frame. The former includes also the contribution from the instantaneous term [Eq. (19)]. Calculation of the nuclear wave function on the light-front is out of the scope of the present paper. Our main focus in the following sections will be the calculation of the electromagnetic current of Eq. (19).

B. Propagating and instantaneous components of electromagnetic current

To identify the propagating and instantaneous parts of the electromagnetic current in Eq. (19) we consider first the electromagnetic vertex $\Gamma^\mu_{\gamma^* N}$. Since the final state of the interacting nucleon is on mass shell, and only the positive light-front energy projections enter in the amplitude, we are led to the half-off-shell vertex function in the general form (see, e.g., Refs. [44–46]:

$$\Gamma^\mu_{\gamma^* N} = \gamma^\mu F_1 + i\sigma^{\mu\nu}q_\nu F_2\frac{\kappa}{2m_N} + q^\mu F_3, \tag{20}$$

where the form-factors $F_{1,2,3} = F_{1,2,3}(m_N^2, p_i^2, q^2)$ are functions of Lorentz invariants constructed from the momenta of initial and final nucleons and momentum transfer q. In general one expects $F_{1,2}(m_N^2, p_i^2, q^2)$ not to be identical with the corresponding on-shell nucleon form factors $[F_{1,2}(m_N^2, m_N^2, q^2)]$. This difference is due to the modification of the internal structure of nucleons in the nuclear medium. Such modification, in principle, should originate from the dynamics similar to the one responsible for the medium modification of partonic distributions of bound nucleon, commonly referred as the EMC effect [47]. This, however, is out of the scope of our discussion since we are interested only in the effects related to the off-shellness of the interacting nucleon's electromagnetic current. Thus, in the numerical estimates we will use unmodified nucleon form factors measured for free nucleons. Concerning F_3, it does not contribute to the cross section of the process due to the gauge invariance of the leptonic current: $q_\mu j_e^\mu = 0$. However, for consistency one can estimate the F_3 form factor based on the fact that due to the conservation of the momentum sum rule in the light-front approach the electromagnetic current of the bound nucleon is conserved:

$$q_\mu J^\mu_N = 0. \tag{21}$$

Using Eq. (19) together with (20) one obtains: $F_3 = F_1\frac{\not{q}}{Q^2}$. Inserting the latter into Eq. (20) one can separate the propagating and instantaneous parts of the electromagnetic vertex in the form

$$\Gamma^{({\rm prop})\mu}_{\gamma^* N} = \gamma^\mu F_1 + i\sigma^{\mu\nu}q_\nu F_2\frac{\kappa}{2m_N}, \tag{22}$$

and

$$\Gamma^{({\rm inst})\mu}_{\gamma^* N} = \left(\gamma^\mu F_1 + i\sigma^{\mu\nu}q_\nu F_2\frac{\kappa}{2m_N}\right)\frac{\Delta\not{p}_i}{2m_N} - F_1\frac{q^\mu}{q^2}\not{q}\left(\mathbf{1} + \frac{\Delta\not{p}_i}{2m_N}\right), \tag{23}$$

where, $\Delta p_i^\mu = p_i^\mu - p_{i,\rm on}^\mu$ and $2\Delta\not{p}_i = \gamma^+(p_i^- - p_{i,\rm on}^-)$ since $\Delta p_i^+ = \Delta p_i^\perp = 0$. In the following derivations we will use the relation:

$$\Delta p_i^- = -q^- + (p_f^- - p_{i,\rm on}^-) = \frac{Q^2}{q^+} - \frac{m_N^2 + \mathbf{p_T}^2}{p_f^+ p_i^+}q^+ = \frac{1}{p_d^+}\left(M_d^2 - 4\frac{(m_N^2 + \mathbf{p_T}^2)}{\alpha(2-\alpha)}\right), \tag{24}$$

as well as:

$$2\Delta p_i \cdot p_i = \Delta p_i^- p_i^+ = p_i^2 - m_N^2, \tag{25}$$

which allow us to express the electromagnetic current in boost-invariant variables.

The separation of the electromagnetic vertex into propagating and instantaneous parts in Eqs. (22) and (23) allows us to separate the electromagnetic current in Eq. (19) into corresponding parts in the following form:

$$J^\mu_N(p_f s_f, p_i s_i) = J^\mu_{\rm prop}(p_f s_f, p_i s_i) + J^\mu_{\rm inst}(p_f s_f, p_i s_i), \tag{26}$$

where,

$$J^\mu_{\rm prop}(p_f s_f, p_i s_i) = \bar{u}(p_f s_f)\Gamma^{({\rm prop})\mu}_{\gamma^* N}u(p_i s_i)$$
$$J^\mu_{\rm inst}(p_f s_f, p_i s_i) = \bar{u}(p_f s_f)\Gamma^{({\rm inst})\mu}_{\gamma^* N}u(p_i s_i). \tag{27}$$

It is worth mentioning that even though the propagating vertex in Eq. (22) has the same form as the free on-shell nucleon vertex the corresponding electromagnetic current $J^{\mu}_{\rm prop}$ does not correspond to an on-shell scattering amplitude, since $q^{\mu} \neq p^{\mu}_{f} - p^{\mu}_{i,\rm on}$. Also, the current conservation [Eq. (21)] is satisfied only for the sum of the propagating and instantaneous currents in Eq. (26).

C. Off-shell parameter of $eN_{\rm bound}$ scattering

While the off-shell effects in the propagating vertex of Eq. (22) are kinematical, due to the fact that $q^{\mu} \neq p^{\mu}_{f} - p^{\mu}_{i,\rm on}$, the off-shell effects in the instantaneous vertex are dynamical. The latter interaction arises exclusively due to the binding of the nucleon. As it follows from Eq. (23) the strength of the instantaneous vertex is proportional to the magnitude of the factor Δp_i^- defined in Eq. (24). One can express the Δp_i^- factor through boost-invariant quantities by defining the light-front reference frame such that the four-momenta of the deuteron, p^{μ}_{d} and momentum transfer q^{μ} are:

$$p^{\mu}_{d} = \left(\frac{Q^2}{m_N}, \frac{m_d^2 m_N}{Q^2}, \mathbf{0_T}\right)$$

$$q^{\mu} = \left(-\frac{Q^2 x}{m_N\left(1+\sqrt{1+\frac{4m_N^2x^2}{Q^2}}\right)}, \frac{m_N}{x}\left(1+\sqrt{1+\frac{4m_N^2x^2}{Q^2}}\right), \mathbf{0_T}\right). \quad (28)$$

Using above definitions one introduces the off-shell parameter η such that,

$$\Delta p_i^- = -m_N \eta, \quad (29)$$

where,

$$\eta = \frac{1}{Q^2}\left(4\frac{(m_N^2 + \mathbf{p_T}^2)}{\alpha(2-\alpha)} - m_d^2\right). \quad (30)$$

As it will be shown in the derivations bellow, the parameter η provides the universal measure of the off-shell effect, which combines both the resolution of the probe through the Q^2 and the binding effects of the nucleon through the light-cone variables, α and $\mathbf{p_T}$.

IV. ELECTRON-NUCLEON SCATTERING CROSS SECTION

In many practical applications one needs to evaluate the electron–bound-nucleon cross section σ_{eN} as it is defined in Ref. [32]. Such a cross section is calculated within PWIA in which case using Eq. (18) the nuclear electromagnetic tensor of Eq. (6) can be expressed as follows:

$$H^{\mu\nu} = H_N^{\mu\nu}(p_f, p_i)\, \rho_d(\alpha, \mathbf{p_T})\, \frac{2-\alpha}{\alpha^2}\, 2(2\pi)^3, \quad (31)$$

where spin-averaged light-cone density matrix of the deuteron $\rho_d(\alpha, p_T)$ and bound-nucleon electromagnetic tensor $H_N^{\mu\nu}(p_f, p_i)$ are defined in the following forms:

$$\rho_d(\alpha, \mathbf{p_T}) = \frac{1}{2s_d+1} \cdot \frac{1}{2} \sum_{s_d, s_i, s_r} \frac{\left|\psi_{\rm LF}^{s_i s_r s_d}(\alpha, \mathbf{p_T})\right|^2}{2-\alpha} \quad (32)$$

and

$$H_N^{\mu\nu} = \frac{1}{2} \sum_{s_i s_f = -1/2}^{1/2} J_N^{\nu}(p_f s_f, p_i s_i)^{\dagger} J_N^{\mu}(p_f s_f, p_i s_i). \quad (33)$$

Inserting now Eq. (31) into Eq. (4) the Lorentz invariant cross section of the reaction (1) can be presented as follows:

$$\frac{d\sigma}{d^3k_f/\epsilon_f d^3p_f/E_f}$$

$$= \frac{1}{2p_d\cdot k_i}\frac{\alpha_{EM}^2}{q^4} L_{\mu\nu} H_N^{\mu\nu}\, \rho_d(\alpha, \mathbf{p_T}) \frac{2-\alpha}{\alpha^2} \delta\left(p_r^2 - m_N^2\right), \quad (34)$$

where $\alpha_{EM} = e^2/(4\pi)$. Introducing the light-front nuclear spectral function in the form:

$$S_d^{\rm LF}(\alpha, \mathbf{p_T}) = \rho_d(\alpha, \mathbf{p_T}) \frac{2-\alpha}{\alpha^2} \delta\left(p_r^2 - m_N^2\right), \quad (35)$$

similar to Ref. [32] one can present the differential cross section as a product of σ_{eN} and the spectral function as follows:

$$\frac{d\sigma}{d\epsilon_f d\Omega_{k_f} d^3p_f} = \sigma_{eN}\, S_d^{\rm LF}(\alpha, \mathbf{p_T}), \quad (36)$$

where

$$\sigma_{eN} = \frac{1}{2m_D\epsilon_i}\frac{\epsilon_f}{E_f}\frac{\alpha_{EM}^2}{q^4} L_{\mu\nu} H_N^{\mu\nu}. \quad (37)$$

Here ϵ_i, ϵ_f are initial and scattered electron energies. The E_f represents the energy of the knock-out nucleon.

It is worth mentioning that the expression in Eq. (36) is universal for any nuclei in which case one needs to replace the deuteron spectral function by the light-front spectral function of the nucleus being considered.

A. Structure functions of bound nucleon

In calculating σ_{eN} in Eq. (37) it is convenient to present it through the four independent structure functions of the nucleon w_L^N, w_{TL}^N, w_T^N, and w_{TT}^N in the form:

$$\sigma_{eN} = \frac{1}{2m_D E_f}\, \sigma_{\rm Mott}\left(v_L w_L^N + v_{TL} w_{TL}^N \cos\phi + v_T w_T^N + v_{TT} w_{TT}^N \cos(2\phi)\right), \quad (38)$$

where $\sigma_{\rm Mott} = \frac{\alpha^2\cos(\frac{\theta}{2})^2}{4\epsilon_i^2\sin(\frac{\theta}{2})^4}$ with θ being scattered electron angle. In the above equation:

$$v_L = \frac{Q^4}{\mathbf{q}^4} \quad v_T = \frac{Q^2}{2\mathbf{q}^2} + \tan^2\frac{\theta}{2}$$

$$v_{TT} = \frac{Q^2}{2\mathbf{q}^2} \quad v_{TL} = \frac{Q^2}{\mathbf{q}^2}\left(\frac{Q^2}{\mathbf{q}^2} + \tan^2\frac{\theta}{2}\right)^{1/2}, \quad (39)$$

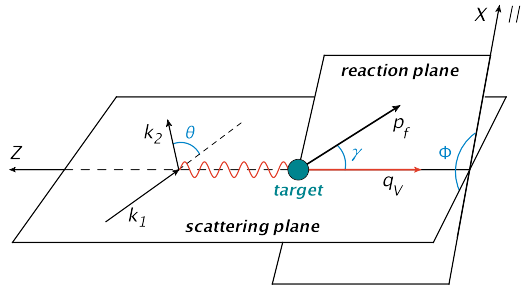

FIG. 4. Definition of scattering and reaction planes of knock-out reaction.

where $Q^2 = 4\epsilon_i\epsilon_f \sin(\frac{\theta}{2})^2$, and $\mathbf{q}$ is the three-momentum of the virtual photon. The above-defined structure functions of the bound nucleon can be related to the light-front components of the nucleonic electromagnet tensor as follows (see Appendix B):

$$
\begin{aligned}
w_L^N &= \frac{\mathbf{q}^2}{4Q^2}\left(H^{++}\frac{Q^2}{(q^+)^2} + 2H^{+-} + \frac{(q^+)^2}{Q^2}H^{--}\right)\\
w_{TL}^N &= \frac{|\mathbf{q}|}{q^+}\left(H_N^{+\parallel} + H_N^{-\parallel}\frac{(q^+)^2}{Q^2}\right)\\
w_T^N &= H_N^{\parallel\parallel} + H_N^{\perp\perp}\\
w_{TT}^N &= H_N^{\parallel\parallel} - H_N^{\perp\perp},
\end{aligned}
\tag{40}
$$

where $\pm$ correspond to $t \pm \hat{z}$ directions on the light cone with $\hat{z}$ defined in the negative direction of of the transferred three-momentum $\mathbf{q}$. The transverse components are chosen as follows: the perpendicular direction is defined by $\mathbf{n}_\perp = \frac{\mathbf{p}_f\times\mathbf{q}}{|\mathbf{p}_f\times\mathbf{q}|}$, and the parallel unit vector projection is $\mathbf{n}_\parallel = \frac{\mathbf{q}\times\mathbf{n}_\perp}{|\mathbf{q}\times\mathbf{n}_\perp|}$. The scattering and reaction planes of the reaction are defined in Fig. 4.

Using now the Eq. (33) and the expression of the bound nucleon electromagnetic current from Eqs. (26) and (27) one can calculate nucleon structure functions explicitly. In what follows we split the structure functions into two terms:

$$
w_i^N = w_{i,\text{prop}}^N + w_{i,\text{inst}}^N \quad \text{for } i = L, TL, T, TT, \tag{41}
$$

where subscript "prop" corresponds to the structure functions calculated using the propagating part of the electromagnetic current, J^μ_{prop} only, while the terms with the subscript "inst" correspond to the contribution from J^μ_{inst} and its interference with J^μ_{prop}.

Using the explicit forms of the currents from Eqs. (26) (27) we calculate the above structure functions expressing them through the off-shell parameter η [Eq. (30)] as follows:[1]

$$
\begin{aligned}
w^N_{\text{L prop}} &= \mathbf{q}^2\left[F_1^2\tau^{-1}\left(1+\frac{p_{\mathbf{T}}^2}{m_N^2}+\tau\eta_i(\eta_i+\eta_q)\right) - F_1F_2\kappa(2+\eta_q) + F_2^2\kappa^2\left(\frac{p_{\mathbf{T}}^2}{m_N^2}+\tau(1+\eta_q)\right)\right],\\
w^N_{\text{L inst}} &= \mathbf{q}^2\left[F_1^2\eta_i(\tau\eta_i(1+\eta_q)-2-\eta_q) + F_1F_2\kappa(\tau\eta_i(2-2\eta_i-\eta_q)+\eta_q) + F_2^2\kappa^2\tau(\tau\eta_i(\eta_i+\eta_q)-\eta_q)\right],\\
w^N_{\text{TL prop}} &= 2\,|\mathbf{q}|\,p_{\mathbf{T}}\left(F_1^2+F_2^2\kappa^2\tau\right)\left[2+4\frac{\alpha_N}{\alpha_q}+2\eta_i+\eta_q\right],\\
w^N_{\text{TL inst}} &= 2|\mathbf{q}|p_{\mathbf{T}}\left(F_1^2+F_2^2\kappa^2\tau\right)(1-\tau\eta_i)\eta_q,\\
w^N_{\text{T prop}} &= 4m_N^2\left[F_1^2\left(\frac{p_{\mathbf{T}}^2}{m_N^2}+2\tau(1+\eta_q)\right) + 2F_1F_2\kappa\tau(2+\eta_q) + F_2^2\kappa^2\tau\left(2+\frac{p_{\mathbf{T}}^2}{m_N^2}+2\tau\eta_i(\eta_i+\eta_q)\right)\right],\\
w^N_{\text{T inst}} &= 2Q^2\left[F_1^2(\tau\eta_i(\eta_i+\eta_q)-\eta_q) + F_1F_2\kappa(\tau\eta_i(2\eta_i+\eta_q-2)-\eta_q) + F_2^2\kappa^2\tau\eta_i(\tau\eta_i(1+\eta_q)-2-\eta_q)\right],\\
w^N_{\text{TT prop}} &= 4p_{\mathbf{T}}^2\left(F_1^2+F_2^2\kappa^2\tau\right),\\
w^N_{\text{TT inst}} &= 0,
\end{aligned}
\tag{42}
$$

where, $\tau = Q^2/(4m_N^2)$, $\eta_i = \eta\,\alpha_N/2$, $\eta_q = \eta\,\alpha_q/2$. Alternatively, one can write,

$$
\eta_i = -\frac{2\Delta p_i\cdot p_i}{Q^2} = \frac{(m_N^2+\mathbf{p_T}^2)}{Q^2}\frac{\alpha_q}{\alpha_f} - \frac{\alpha_N}{\alpha_q}, \tag{43}
$$

$$
\eta_q = -\frac{2\Delta p_i\cdot q}{Q^2} = \frac{(m_N^2+\mathbf{p_T}^2)}{Q^2}\frac{\alpha_q^2}{\alpha_f\alpha_N} - 1. \tag{44}
$$

[1] In Appendix B we also presented the same structure functions in more conventional form in terms of scalar products of kinematical variables describing the reaction [see Eq. (B10)].

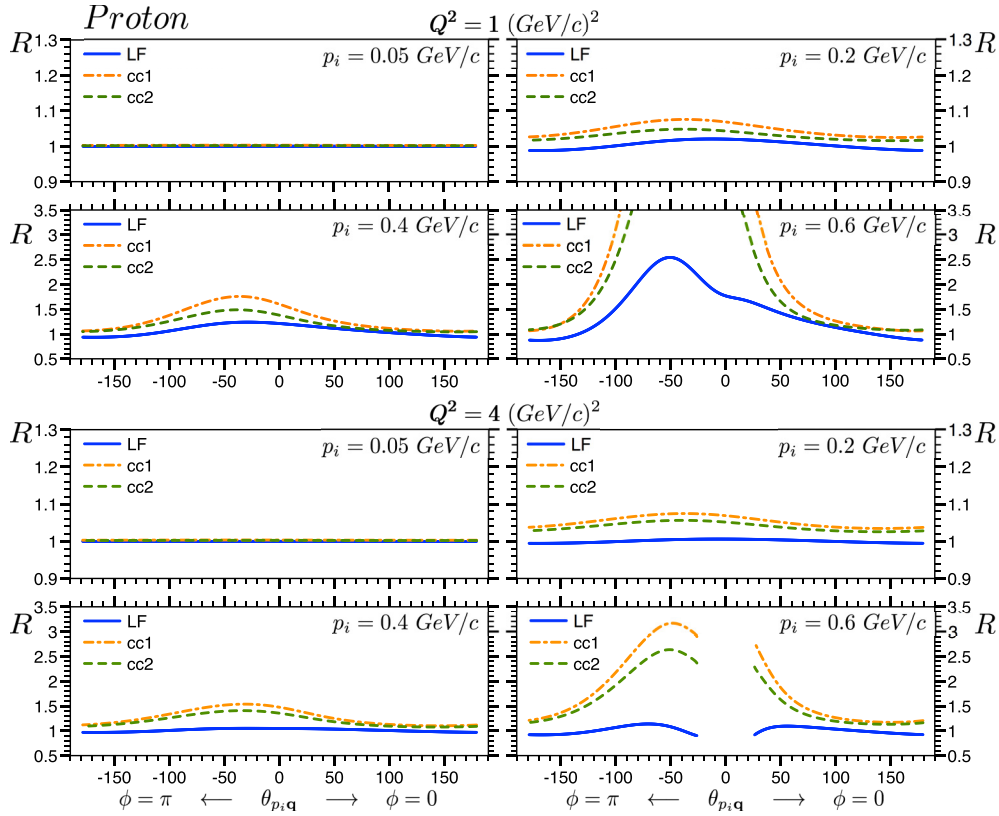

FIG. 5. The $\theta_{p_i q}$ dependence of ratios of the off-shell cross section of electron-bound proton scattering to that of the one-shell cross section. The solid lines are LF approximation, dashed and dash-dotted curves corresponds to CC2 and CC1 versions of de Forest approximation [32]. The panels correspond to the bound nucleon momenta $p_i = 50, 200, 400$, and 600 MeV/c for $Q^2 = 1$ and 4 $(\mathrm{GeV/c})^2$. The minus sign of θ_{pq} indicates on kinematics corresponding to $\phi = 180^\circ$ between scattering and reaction planes. Calculations done for initial electron energy $\epsilon_i = 11$ GeV.

The structure functions in Eq. (42) are Lorentz invariant and expressed through the boost-invariant variables η, α_i, α_q, and α_f. Since many experiments in probing high momentum bound nucleons are performed in the fixed target experiments it is convenient to express the above variables through the four-momenta measured in the laboratory frame. Considering a laboratory reference frame in which $\hat{z} \| \mathbf{q}$, the α_i, α_q, and α_f parameters can be expressed as follows:

$$\alpha_i = 2 - \alpha_r = \alpha_f - \alpha_q, \quad \alpha_r = \frac{2(E_r - p_r \cos\theta_r)}{m_d},$$
$$\alpha_q = \frac{2(q_0 - \mathbf{q})}{m_d}, \quad \alpha_f = \frac{2(E_f - p_f \cos\theta_f)}{m_d}, \tag{45}$$

where, $p_d^\mu = (m_d, 0)$, $q^\mu = (q_0, \mathbf{q})$, $p_r^\mu = (E_r, \mathbf{p_r})$, and $p_f^\mu = (E_f, \mathbf{p_f})$ are four-momenta of the target deuteron, virtual photon, recoil, and struck nucleon measured in the laboratory frame.

V. NUMERICAL ESTIMATES

We present numerical estimates for kinematics, which will be explored in experiments planned for 12 GeV upgraded Jefferson Lab. In all calculations below we take the initial energy of the electron beam $\epsilon_i = 11$ GeV.

To quantify the extent of the binding effects we consider the ratio:

$$R = \frac{\sigma_{eN}}{\sigma_{eN}^{\mathrm{on}}}, \tag{46}$$

where σ_{eN} is the cross section of electron bound nucleon scattering defined in Eq. (37) for given initial momenta $\mathbf{p_i}$ or (α_i and p_T), while $\sigma_{eN}^{\mathrm{on}}$ corresponds to the same cross section for the electron scattering off the free-moving nucleon with the same initial momenta.

First, we consider the dependence of R on traditional kinematical parameters, which define the electronuclear processes such as initial momentum of the bound nucleon (p_i) its relative angle with respect to the transferred three-momentum ($\mathbf{q}$), as well as the virtuality of the transferred momentum (Q^2). Additionally we compare the predictions of LF approximation with that of the de Forest formalism [32], which is commonly used in the analysis of the experimental data. In all these estimates we use the same parametrization for the electric and magnetic form factors of the nucleons. These parametrizations are the same for the free nucleon. Thus we do not consider the effects related to the possible modification of the charge and magnetic current distributions in the bound nucleon.

In Figs. 5 and 6 we compare the angular dependences of ratio R at different values of missing momenta at fixed

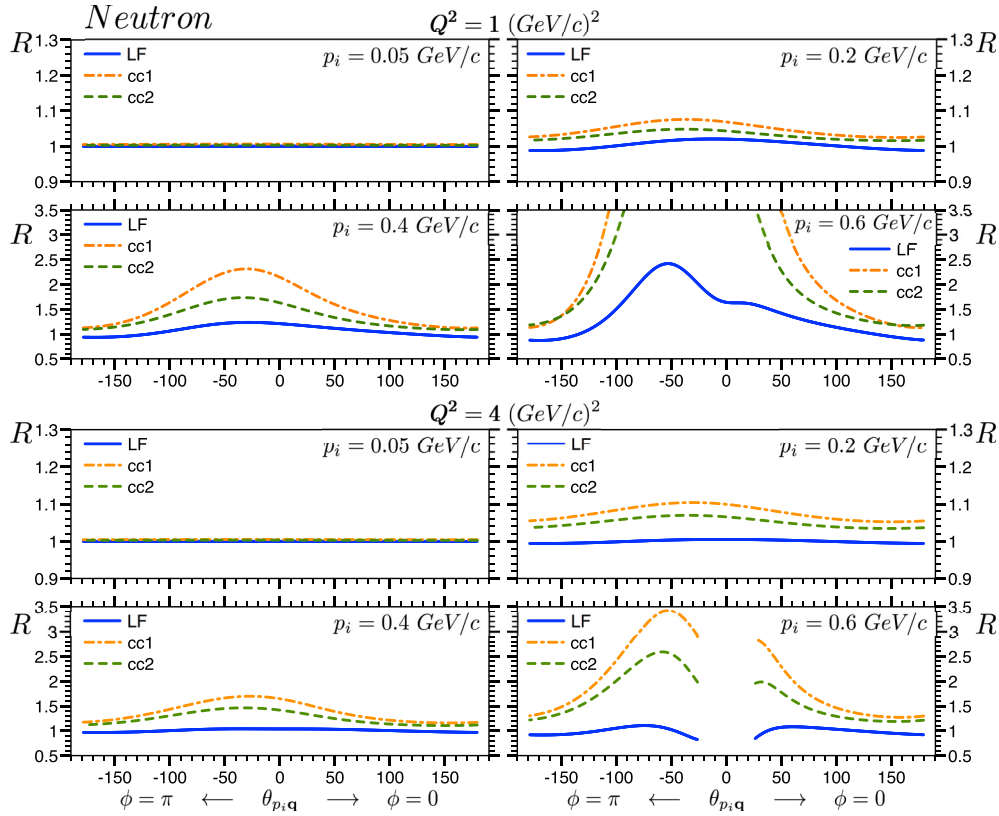

FIG. 6. The same as in Fig. 5 but for scattering from bound neutron.

$Q^2 = 1$ and 4 $(\mathrm{GeV/c})^2$ for bound proton and neutron, respectively. As Fig. 5 shows LF approximation predicts off-shell effects for $Q^2 = 1\,(\mathrm{GeV/c})^2$ as large as 40–250% for bound proton momenta $\geqslant$400 MeV/c. Even larger effects are expected within the de Forest approach [32]. We observe also that the prediction within LF and de Forest approximations significantly diverge close to the kinematical limit of the scattering process as it can be seen in calculations for $p_i = 600$ MeV/c.

Because of different magnitudes and signs of form factors one predicts somewhat different off-shell effects for scattering from a bound proton or neutron. However, qualitatively the dependences of R for kinematical parameters of the reaction for both proton and neutron are similar.

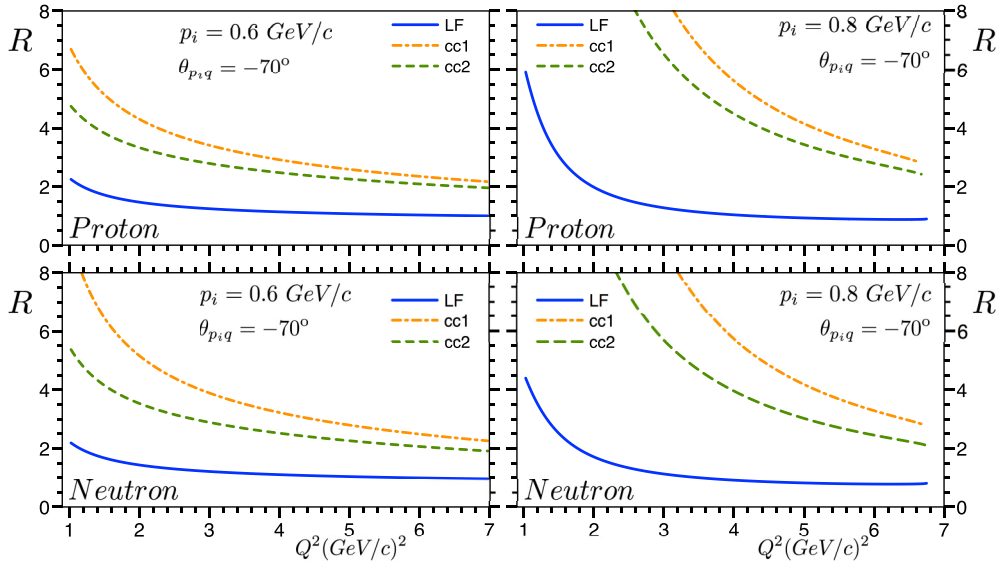

FIG. 7. The Q^2 dependence of the off-shell effects for $\theta_{p_i q} = -70^\circ$ for proton and neutron targets.

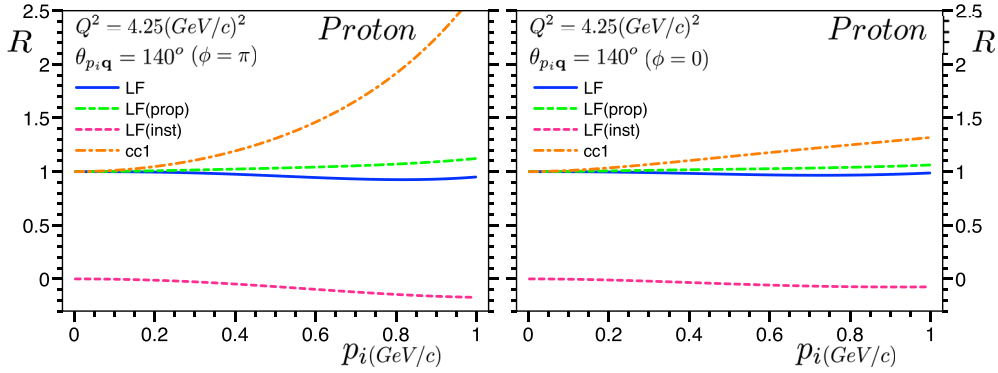

FIG. 8. Off-shell effects expected for the experiment of Ref. [48] (left). The right panel is the similar effects for $\phi = 0$ kinematics.

An important feature of LF calculations following from Figs. 5 and 6 is the diminishing of the off-shell effects with an increase of Q^2. This reflects the dynamical nature of the LF approximation in which case the harder the probe (larger Q^2), the lesser is the sensitivity to the binding effects of the target nucleon. It is worth mentioning that no such behavior exists in the de Forest approximation since in this case part of the off-shell effects are kinematical in which the energy of bound nucleon is taken to be equal to the on-shell energy for the given momentum of the nucleon, with the phase space of the initial nucleon being proportional to $\frac{1}{\sqrt{m_N^2+p_i^2}}$.

To ascertain the extent of the Q^2 suppression on the off-shell effects, in Fig. 7 we present the Q^2 dependence of the ratio R for proton and neutron initial momenta of $p_i = 600$ and 800 MeV/c. Here we choose $\theta_{p_iq} = -70^\circ$ for which large off-shell effects are observed in Figs. 5 and 6. These calculations indicate that already at $Q^2 \geqslant 4$ GeV^2 the off-shell effects predicted in light-front approximation are not more than 10% for such a large bound nucleon momenta.

For practical purposes in Fig. 8 we estimate the dependence of the off-shell effects on the momentum of the bound nucleon for kinematics relevant to the planned JLAB experiment [48], which is aimed at probing deuteron structure at very large internal momenta. As the figure shows for both cases of the angles between scattering and reaction planes (ϕ) the light-front approach predicts off-shell effects to be less than 8% for all kinematics with the latter value happening at $p_i =$ 850 MeV/c.

At the end of the section we discuss whether the parameter η introduced in Eq. (30) can be used as a universal parameter for estimation of the off-shell effects for any kinematic conditions of electroproduction reaction. For this, in Fig. 9 we calculate the η dependence of $|R-1|$ for very large magnitudes of bound nucleon momenta ($p_i = 600$ and 800 MeV/c) at different values of transverse momentum p_T. Note that the expected off-shell effects will be much less for smaller values of p_i.

As Fig. 9 shows for any possible scenarios of kinematics the off-shell effects can be confined below 5% as soon as $\eta < 0.1$. This represents a strong indication that the variable η

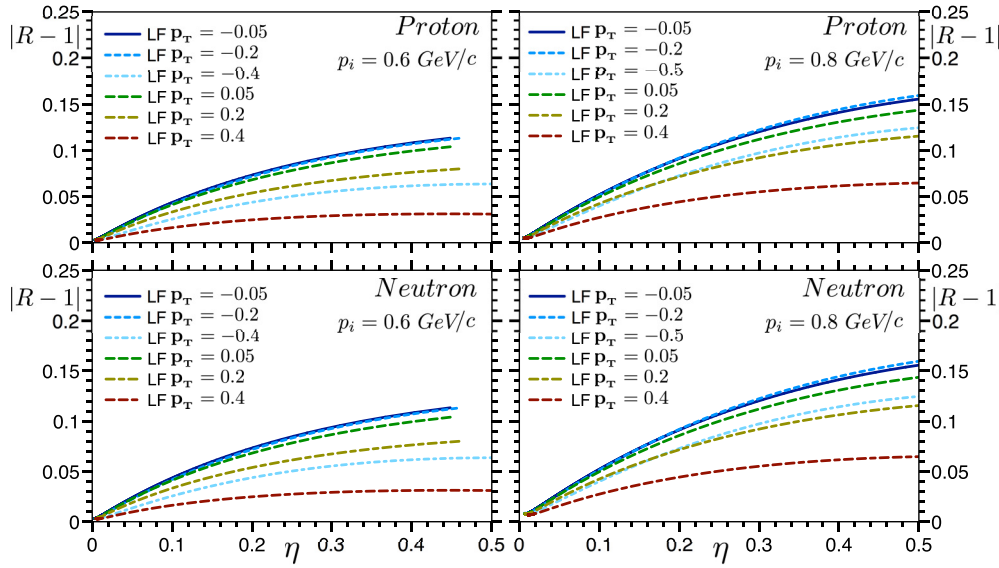

FIG. 9. The η parameter dependence of the off-shell effects $|R-1|$ for $p_i = 0.6$ and 0.8 GeV/c at different values of the transverse momentum p_T.

can be considered as a universal parameter for controlling the off-shell effects in the reaction mechanism of electron-nuclear processes. The universality here is in the fact that, if our goal is to probe a bound nucleon with very large momenta, we can calculate the corresponding α and $p_{\mathbf{T}}$ parameters and then find the required Q^2 such that it makes $\eta < 0.1$, thus allowing us to neglect the off-shell effects in the electromagnetic current.

VI. SUMMARY AND OUTLOOK

Based on the light-front approach we calculated electron-deuteron scattering within PWIA, which allowed us to isolate the electron–bound-nucleon scattering cross section, σ_{eN}. Within LF approximation the vacuum contribution naturally disappears while the off-shell nature of the nucleon results in an appearance of an instantaneous term in the electromagnetic current of electron–bound-nucleon scattering. In deriving σ_{eN} we separated the propagating and instantaneous contributions in the electromagnetic current, which allowed us to trace explicitly the effects associated with the binding of the nucleon. Furthermore, in the LF approach we were able to identify the parameter (defined as η) that universally characterizes the extent of the off-shellness of electromagnetic current.

The derived σ_{eN} is used to estimate the expected off-shell effects in electronuclear processes in kinematics relevant to the 12 GeV energy upgraded Jefferson Lab experiments. We compared the LF predictions with that of the de Forest approximation widely used by experimentalists to estimate the off-shell effects in the reaction mechanism of electronuclear processes. These comparisons indicate that practically in all kinematic cases the LF approach predicts less off-shell effects at $Q^2 \geqslant 1$ GeV^2 than the de Forest approximation does. Most importantly the LF approach predicts a significant drop of the off-shell effects with an increase of Q^2, which intuitively can be understood as a decrease in the sensitivity of the hard processes on the off-shellness of the target nucleon.

We also checked our conjecture that the η variable can be considered as a universal parameter in controlling off-shell effects. We found that for a wide range of kinematics the off-shell effects can be suppressed on the level of 5% as as soon as $\eta < 0.1$. The latter gives an effective method for controlling the uncertainties in the reaction mechanism for large varieties of electronuclear processes probing deeply bound nucleons in the nucleus.

Finally, it is worth mentioning that even though we considered the eA scattering within PWIA the obtained expressions for electromagnetic current are applicable also for scattering amplitudes in which the final-state interaction between outgoing nucleons is considered within eikonal approximation. In this case (see, e.g., Refs. [18,19]) the main part of the rescattering amplitude is evaluated at the pole value of the struck nucleon propagator in the intermediate state. As a result the entered electromagnetic current is again half-off-shell as the considered electromagnetic current in Eq. (26).

ACKNOWLEDGMENTS

We are thankful to Dr. Werner Boeglin and Chris Leon for numerous discussions on the physics of high-energy electronuclear reactions. This work is supported by the US DOE grant under Contract No. DE-FG02-01ER-41172.

APPENDIX A: LIGHT FRONT PERTURBATION THEORY RULES

We present here a summary of the rules for computation of amplitudes within light-front (LF) formalism.

The LF scalar product and notations are (Lepage-Brodsky convention [35,37]):

$$\begin{aligned} x \cdot p &= \tfrac{1}{2}(x^+ p^- + x^- p^+) - \mathbf{x_T} \cdot \mathbf{p_T} \\ x^\mu &= (x^+, x^-, x, y) = (x^+, x^-, \mathbf{x_T}), \\ p^\mu &= (p^+, p^-, \mathbf{p_T}) \\ x^\pm &= t \pm z. \end{aligned} \tag{A1}$$

Diagrammatic rules for effective light-front perturbation theory can be formulated as follows:

(i) Draw all topologically distinct $\tau \equiv x^+$-ordered diagrams at the desired coupling power. In addition to the usual advanced and retarded propagation between two events one needs to include a third possibility in which the two events connected by an internal fermion or photon interact at the same LF τ time, commonly referred as instantaneous term.

(ii) Assign to each line a four-momentum p^μ and spin s (or helicity λ) corresponding to a single on-mass-shell particle, i.e., $p^2 = m^2$.

(iii) With spin-1/2 fermions associate on-mass-shell spinors $u(p, s)$, with antifermions $v(p, s)$, with photons $\epsilon_\mu(q, \lambda)$, etc., such that,

$$\begin{aligned} \bar{u}(p, s')u(p, s) &= -\bar{v}(p, s')v(p, s) = 2m\delta_{ss'} \\ \sum_s u(p, s)\bar{u}(p, s) &= \not{p} + m \\ \sum_s v(p, s)\bar{v}(p, s) &= \not{p} - m \\ \epsilon^\mu(q, \lambda')\epsilon^\mu(q, \lambda) &= -\delta_{\lambda'\lambda}\,, \quad q \cdot \epsilon(q, \lambda) = 0 \\ \sum_\lambda \epsilon^\mu(q, \lambda)\epsilon^\nu(q, \lambda) &= -g^{\mu\nu} + \frac{q^\mu \eta^\nu + q^\nu \eta^\mu}{q \cdot \eta}, \end{aligned} \tag{A2}$$

where η is a null vector ($\eta^2 = 0$), given in LC gauge by, $\eta = (0, 2, 0, 0)$.

(iv) Each intermediate state gets a factor (inverse of the difference of the sums over initial and intermediate LF energies p_-):

$$\frac{1}{\sum_{\text{ini}} p^- - \sum_{\text{int}} p^- + i\epsilon}, \tag{A3}$$

where, ini stands for the initial state of the diagram and int for intermediate states. All particles are on-mass-shell, that is: $p^- = \frac{m^2 + p_{\mathbf{T}}^2}{p_i^+} > 0$.

(v) Internal lines account for two kind of interactions:
(1) Propagating, in which case, for a vertex like in Fig. 10(a) one has:

$$\Gamma\,\bar{u}(p',s')\not{\epsilon}(q,\lambda)u(p,s)\delta^2\left(\sum_{\text{in}} p_{\mathbf{T}}-\sum_{\text{out}} p_{\mathbf{T}}\right)\times\delta\left(\sum_{\text{in}} p^+-\sum_{\text{out}} p^+\right), \tag{A4}$$

where, in and out mean flowing into and out of the vertex. The δ functions at the vertex provide an explicit conservation of the plus and transverse components of in and out momenta.

(2) Instantaneous. For each vertex like in Fig. 10(b) (fermionic), include,

$$\Gamma^2\,\bar{u}(p',s')\not{\epsilon}(q',\lambda')\frac{\gamma^+}{2(q^+-p'^+)}\not{\epsilon}(q,\lambda)u(p,s)\times\delta^2\left(\sum_{\text{in}} p_{\mathbf{T}}-\sum_{\text{out}} p_{\mathbf{T}}\right)\delta\left(\sum_{\text{in}} p^+-\sum_{\text{out}} p^+\right) \tag{A5}$$

and, for each vertex like in Fig. 10(c) (vector), include,

$$\Gamma^2\,\bar{u}(p',s')\gamma^+u(p,s)\frac{1}{(p'^+-p^+)^2}\bar{u}(k',\sigma')\times\gamma^+u(k,\sigma)\delta^2\left(\sum_{\text{in}} p_{\mathbf{T}}-\sum_{\text{out}} p_{\mathbf{T}}\right)\times\delta\left(\sum_{\text{in}} p^+-\sum_{\text{out}} p^+\right). \tag{A6}$$

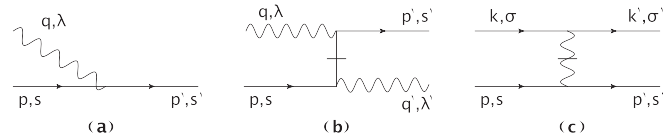

FIG. 10. Example of the scattering amplitude on the light-front ($\tau = x^+$ flows from left to right).

Here Γ factors represent effective vertices, which can be specified for the particular case of the scattering. They can correspond to electron–bound-nucleon scattering as well as nuclear transition to the constituent nucleons. The conditions for for which such an effective vertices can be introduced in the Feynman diagrams are discussed in Ref. [19].

(vi) Sum over polarizations and integrate over each internal line with the factor,

$$\sum_s\int\frac{dp_{\mathbf{T}}dp^+}{2(2\pi)^3p^+}\Theta(p^+),$$

which ensures the plus component positivity (all particles move forward in LC time).

(vii) Include symmetry factors. Also, a factor of -1 for each fermion loop, for fermion lines beginning and ending at the initial state, and for each diagram in which fermion lines are interchanged in either of the initial or final states, as well as the overall sign from Wick's theorem.

APPENDIX B: NUCLEONIC TENSOR

Substituting Eq. (26) into Eq. (33), allows us to express the nucleonic tensor as a sum of two terms:

$$H_N^{\mu\nu}=H_{N\,\text{prop}}^{\mu\nu}+H_{N\,\text{inst}}^{\mu\nu}, \tag{B1}$$

where the propagating contribution is given by,

$$H_{N\,\text{prop}}^{\mu\nu}=\frac{1}{2}\sum_{s_is_f}\left(J_{\text{prop}}^{s_is_f\,\mu}\right)^\dagger\left(J_{\text{prop}}^{s_is_f}\right)^\nu=\frac{1}{2}\text{Tr}\left[\overline{\Gamma}^{(\text{on})\mu}_{\gamma^*N}(\not{p}_f+m_N)\Gamma^{(\text{on})\nu}_{\gamma^*N}(\not{p}_{i,\text{on}}+m_N)\right], \tag{B2}$$

and the instantaneous by,

$$\begin{aligned}H_{N\,\text{inst}}^{\mu\nu}&=\frac{1}{2}\sum_{s_is_f}\left(\left(J_{\text{off}}^{s_is_f\,\nu}\right)^\dagger J_{\text{inst}}^{s_is_f\,\mu}+\left(J_{\text{prop}}^{s_is_f\,\nu}\right)^\dagger J_{\text{inst}}^{s_is_f\,\mu}+\left(J_{\text{inst}}^{s_is_f\,\nu}\right)^\dagger J_{\text{prop}}^{s_is_f\,\mu}\right)\\&=\frac{1}{2}\text{Tr}\left[\overline{\Gamma}^{(\text{off})\nu}_{\gamma^*N}(\not{p}_f+m_N)\Gamma^{(\text{off})\mu}_{\gamma^*N}(\not{p}_{i,\text{on}}+m_N)+\overline{\Gamma}^{(\text{on})\nu}_{\gamma^*N}(\not{p}_f+m_N)\Gamma^{(\text{off})\mu}_{\gamma^*N}(\not{p}_{i,\text{on}}+m_N)\right.\\&\quad\left.+\overline{\Gamma}^{(\text{off})\nu}_{\gamma^*N}(\not{p}_f+m_N)\Gamma^{(\text{on})\mu}_{\gamma^*N}(\not{p}_{i,\text{on}}+m_N)\right],\end{aligned} \tag{B3}$$

where, $\overline{\Gamma}^\mu_{\gamma^*N}=\gamma^0(\Gamma^\mu_{\gamma^*N})^\dagger\gamma^0$. Notice that the initial momentum of the nucleon, p_i, occurring from now on corresponds to $p_{i,\text{on}}$, which allows to drop the on-shell label "on" without confusion. With this, we can write propagating and instantaneous

contributions of the tensor, $H^{\mu,\nu}$ as functions of the nucleon form factors F_1 and F_2 as follows:

$$\begin{aligned} H^{\mu\nu}_{N\ \mathrm{prop}} = {} & 2F_1^2\big[g^{\mu\nu}\big(m_N^2 - p_i\cdot p_f\big) + \big(p_i^\mu p_f^\nu + p_i^\nu p_f^\mu\big)\big] + F_1F_2\kappa\big[2g^{\mu\nu}q\cdot(p_f-p_i) + \big(p_i^\mu q^\nu + p_i^\nu q^\mu\big) - \big(p_f^\mu q^\nu + p_f^\nu q^\mu\big)\big] \\ & + F_2^2\frac{\kappa^2}{2m_N^2}\big[g^{\mu\nu}\big[q^2\big(p_i\cdot p_f + m_N^2\big) - 2\,q\cdot p_i\,q\cdot p_f\big] - q^2\big(p_i^\mu p_f^\nu + p_i^\nu p_f^\mu\big) \\ & - q^\mu q^\nu\big(p_i\cdot p_f + m_N^2\big) + q\cdot p_f\big(p_i^\mu q^\nu + p_i^\nu q^\mu\big) + q\cdot p_i\big(p_f^\mu q^\nu + p_f^\nu q^\mu\big)\big], \end{aligned} \tag{B4}$$

and the instantaneous correction as follows:

$$\begin{aligned} H^{\mu\nu}_{N\ \mathrm{inst}} = {} & 2F_1^2\Bigg[g^{\mu\nu}\bigg(\Delta p_i\cdot(p_i-p_f) - \frac{\Delta p_i\cdot p_i}{m_N^2}\Delta p_i\cdot p_f\bigg) + \big(\Delta p_i^\mu p_f^\nu + \Delta p_i^\nu p_f^\mu\big)\bigg(1+\frac{\Delta p_i\cdot p_i}{m_N^2}\bigg) \\ & + \frac{2}{q^2}q^\mu q^\nu\bigg(\frac{2}{q^2}q\cdot p_f\,q\cdot(\Delta p_i+p_i) - (p_i-p_f)\cdot(\Delta p_i+p_i) + \frac{\Delta p_i\cdot p_i}{m_N^2}\bigg(\frac{\Delta p_i\cdot q}{q^2}p_f\cdot q + \Delta p_i\cdot p_f\bigg)\bigg) \\ & - \frac{2}{q^2}\big(p_i^\mu q^\nu + p_i^\nu q^\mu\big)q\cdot p_f - \frac{2}{q^2}\big(p_f^\mu q^\nu + p_f^\nu q^\mu\big)\bigg(q\cdot(\Delta p_i+p_i) + \frac{\Delta p_i\cdot p_i}{m_N^2}\Delta p_i\cdot q\bigg) \\ & - \frac{2}{q^2}\big(\Delta p_i^\mu q^\nu + \Delta p_i^\nu q^\mu\big)q\cdot p_f\bigg(1+\frac{\Delta p_i\cdot p_i}{m_N^2}\bigg)\Bigg] + F_1F_2\kappa\Bigg[g^{\mu\nu}\bigg(\frac{\Delta p_i\cdot p_i}{m_N^2}q\cdot(2p_f-\Delta p_i) - 2\Delta p_i\cdot q\bigg) \\ & + q^\mu q^\nu\bigg(\frac{\Delta p_i\cdot p_i}{m_N^2q^2}q\cdot(\Delta p_i - 2p_f) - 2\bigg) - \big(p_i^\mu q^\nu + p_i^\nu q^\mu\big) + \big(p_f^\mu q^\nu + p_f^\nu q^\mu\big)\Bigg] \\ & + F_2^2\frac{\kappa^2}{2m_N^2}\Bigg[g^{\mu\nu}\bigg[(q^2\,\Delta p_i\cdot p_f - 2\,q\cdot\Delta p_i\,q\cdot p_f)\bigg(1+\frac{\Delta p_i\cdot p_i}{m_N^2}\bigg) + q^2\,\Delta p_i\cdot p_i\bigg] \\ & - \big(\Delta p_i^\mu p_f^\nu + \Delta p_i^\nu p_f^\mu\big)q^2\bigg(1+\frac{\Delta p_i\cdot p_i}{m_N^2}\bigg) - q^\mu q^\nu\bigg[\Delta p_i\cdot p_f\bigg(1+\frac{\Delta p_i\cdot p_i}{m_N^2}\bigg) - \Delta p_i\cdot p_i\bigg] \\ & + \big(\Delta p_i^\mu q^\nu + \Delta p_i^\nu q^\mu\big)q\cdot p_f\bigg(1+\frac{\Delta p_i\cdot p_i}{m_N^2}\bigg) + \big(p_f^\mu q^\nu + p_f^\nu q^\mu\big)q\cdot\Delta p_i\bigg(1+\frac{\Delta p_i\cdot p_i}{m_N^2}\bigg)\Bigg]. \end{aligned} \tag{B5}$$

With our choice of reference frame [Fig. (4)], one can expand the $L_{\mu\nu}H^{\mu\nu}$ product in the following form:

$$\begin{aligned} L_{\mu\nu}H_N^{\mu\nu} = {} & (L_{00}H^{00} - 2L_{0z}H^{0z} + L_{zz}H^{zz}) + (-2L_{0\parallel}H^{0\parallel} + 2L_{z\parallel}H^{z\parallel}) \\ & + \tfrac{1}{2}(L_{\parallel\parallel} + L_{\perp\perp})(H^{\parallel\parallel} + H^{\perp\perp}) + \tfrac{1}{2}(L_{\parallel\parallel} - L_{\perp\perp})(H^{\parallel\parallel} - H^{\perp\perp}). \end{aligned} \tag{B6}$$

Furthermore, using the gauge invariance of leptonic current, one expresses the above product in the form:

$$\begin{aligned} L_{\mu\nu}H_N^{\mu\nu} = {} & L_{00}\bigg(H^{00} - 2\frac{q^0}{q_z}H^{0z} + \bigg(\frac{q^0}{q_z}\bigg)^2H^{zz}\bigg) + 2L_{0\parallel}\bigg(-H^{0\parallel} + \frac{q^0}{q_z}H^{z\parallel}\bigg) \\ & + \frac{1}{2}(L_{\parallel\parallel} + L_{\perp\perp})(H^{\parallel\parallel} + H^{\perp\perp}) + \frac{1}{2}(L_{\parallel\parallel} - L_{\perp\perp})(H^{\parallel\parallel} - H^{\perp\perp}) \\ = {} & Q^2[\tan(\theta/2)]^2\big(v_Lw_L^N + v_{TL}w_{TL}^N\cos(\phi) + v_Tw_T^N + v_{TT}w_{TT}^N\big). \end{aligned} \tag{B7}$$

Using the definitions of v_i for $i = L, T, TL, TT$ from Eq. (39), for the hadronic structure functions w_i^N, one obtains:

$$\begin{aligned} w_L^N &= \frac{\mathbf{q}^4}{Q^4}\bigg(H^{00} - 2\frac{q^0}{q_z}H^{0z} + \frac{(q^0)^2}{\mathbf{q}^2}H^{zz}\bigg) = \frac{\mathbf{q}^2}{4Q^2}\bigg(H^{++}\frac{Q^2}{(q^+)^2} + 2H^{+-} + \frac{(q^+)^2}{Q^2}H^{--}\bigg) \\ w_{TL}^N &= 2\frac{\mathbf{q}^2}{Q^2}\bigg(\frac{q^0}{q_z}H_N^{z\parallel} - H_N^{0\parallel}\bigg) = \frac{|\mathbf{q}|}{q^+}\bigg(H_N^{+\parallel} + H_N^{-\parallel}\frac{(q^+)^2}{Q^2}\bigg) \\ w_T^N &= H_N^{\parallel\parallel} + H_N^{\perp\perp} \\ w_{TT}^N &= H_N^{\parallel\parallel} - H_N^{\perp\perp}, \end{aligned} \tag{B8}$$

where we have used, $-q_z = |\mathbf{q}|$, as well as the relation between components of the nucleonic tensor in light-cone and Minkowski coordinates:

$$\begin{aligned} H^{00} &= \tfrac{1}{4}(H^{++} + 2H^{+-} + H^{--}) \\ H^{0z} &= \tfrac{1}{4}(H^{++} - H^{--}) \\ H^{zz} &= \tfrac{1}{4}(H^{++} - 2H^{+-} + H^{--}) \\ H^{0\parallel} &= \tfrac{1}{2}(H^{+\parallel} + H^{-\parallel}) \\ H^{z\parallel} &= \tfrac{1}{2}(H^{+\parallel} - H^{-\parallel}). \end{aligned} \tag{B9}$$

From Eqs. (B4) and (B8) we compute the explicit forms of the structure functions. In the reference frame of Fig. 4, they are given by:

$$\begin{aligned} w^N_{\mathrm{L\ prop}} &= F_1^2\mathbf{q}^2\frac{\alpha_N\alpha_f}{\alpha_q^2}\left(\frac{m_N^2+p_{\mathbf{T}}^2}{Q^2}\frac{\alpha_q^2}{\alpha_N\alpha_f}+1\right) - F_1F_2\mathbf{q}^2\kappa\left(\frac{m_N^2+p_{\mathbf{T}}^2}{Q^2}\frac{\alpha_q^2}{\alpha_N\alpha_f}+1\right) \\ &\quad + F_2^2\mathbf{q}^2\left(\frac{\kappa}{2m_N}\right)^2\left((m_N^2+p_{\mathbf{T}}^2)\frac{\alpha_q^2}{\alpha_N\alpha_f}+4p_{\mathbf{T}}^2\right) \\ w^N_{\mathrm{L\ inst}} &= F_1^2\frac{\alpha_N}{\alpha_q}\mathbf{q}^2\left(1-\left(\frac{m_N^2+p_{\mathbf{T}}^2}{Q^2}\frac{\alpha_q^2}{\alpha_N\alpha_f}\right)^2+\frac{(m_N^2+p_{\mathbf{T}}^2)}{2m^2}\frac{\alpha_q}{\alpha_N}+\left(\frac{m_N^2+p_{\mathbf{T}}^2}{Q^2}\frac{\alpha_q^2}{\alpha_N\alpha_f}-1\right)^2\right) \\ &\quad - 2F_1F_2\kappa\frac{\alpha_N}{\alpha_q}\mathbf{q}^2\frac{(q\cdot\Delta p_i)^2}{m^2Q^2}\left(2\frac{\alpha_f}{\alpha_q}+2\frac{m^2}{q\cdot\Delta p_i}+1\right)+F_2^2\left(\frac{\kappa}{m_N^2}\right)^2\mathbf{q}^2\,q\cdot\Delta p_i\left(1+\frac{q\cdot\Delta p_i}{m^2}\frac{\alpha_N\alpha_f}{\alpha_q^2}\right) \\ w^N_{\mathrm{TL\ prop}} &= |\mathbf{q}|\frac{\alpha_N+\alpha_f}{\alpha_q}p_{\mathbf{T}}\left(2F_1^2+2F_2^2\left(\frac{\kappa}{2m_N}\right)^2Q^2\right)\left(1+\frac{m_N^2+p_{\mathbf{T}}^2}{Q^2}\frac{\alpha_q^2}{\alpha_N\alpha_f}\right) \\ w^N_{\mathrm{TL\ inst}} &= 8|\mathbf{q}|\frac{q\cdot\Delta p_i}{Q^2}p_{\mathbf{T}}\left(1+\frac{p_i\cdot\Delta p_i}{m^2}\right)\left(F_1^2+F_2^2\left(\frac{\kappa}{2m_N}\right)^2\right) \\ w^N_{\mathrm{T\ prop}} &= F_1^2\left(2(m_N^2+p_{\mathbf{T}}^2)\frac{\alpha_q^2}{\alpha_N\alpha_f}+4(p_{\mathbf{T}})^2\right)+2\kappa F_1F_2\left((m_N^2+p_{\mathbf{T}}^2)\frac{\alpha_q^2}{\alpha_N\alpha_f}+Q^2\right) \\ &\quad + F_2^2\left(\frac{\kappa}{2m_N}\right)^2\left(2\frac{\alpha_N\alpha_f}{\alpha_q^2}\left((m_N^2+p_{\mathbf{T}}^2)\frac{\alpha_q^2}{\alpha_N\alpha_f}+Q^2\right)^2-4Q^2p_{\mathbf{T}}^2\right) \\ w^N_{\mathrm{T\ inst}} &= 8F_1^2\left(q\cdot\Delta p_i+p_f\cdot\Delta p_i\frac{p_i\cdot\Delta p_i}{m^2}\right)+8F_1F_2\kappa\left(1+\frac{p_i\cdot\Delta p_i}{m^2}\right)\left(q\cdot\Delta p_i-p_f\cdot q\frac{p_i\cdot\Delta p_i}{m^2+p_i\cdot\Delta p_i}\right) \\ &\quad + 8F_2^2\left(\frac{\kappa}{2m_N}\right)^2\left(1+\frac{p_i\cdot\Delta p_i}{m^2}\right)\left(q\cdot p_f\,q\cdot\Delta p_i+Q^2\,p_f\cdot\Delta p_i+Q^2\frac{m^2\,p_i\cdot\Delta p_i}{m^2+p_i\cdot\Delta p_i}\right) \\ w^N_{\mathrm{TT\ prop}} &= 4p_{\mathbf{T}}^2\left(F_1^2+F_2^2\frac{\kappa^2}{4m_N^2}Q^2\right) \\ w^N_{\mathrm{TT\ off}} &= 0. \end{aligned} \tag{B10}$$

The kinematic variables and scalar products used in the calculation are as follows: The light-cone momentum fractions are

$$\alpha_N = \frac{2p_N^+}{p_d^+} = \frac{2(E_N+p_{N,z})}{p_d^+}, \quad \alpha_q = \frac{2q^+}{p_d^+} = \frac{2(q^0-|\mathbf{q}|)}{p_d^+}, \quad \alpha_f = \alpha_N+\alpha_q \tag{B11}$$

and the off-shell factor is, $\Delta p_i^\mu = p_i^\mu - p_{i,\mathrm{on}}^\mu$, with, $p_i^\mu = p_d^\mu - p_r^\mu$. Since $\Delta p_i^+ = \Delta p_i^\perp = 0$, we have, $2\Delta\not{p}_i = \gamma^+(p_i^- - p_{i,\mathrm{on}}^-)$ with the minus component defined as follows:

$$\Delta p_i^- = p_i^- - p_{i\ \mathrm{on}}^- = -q^- + (p_f^- - p_{i\ \mathrm{on}}^-) = \frac{Q^2}{q^+} - \frac{m_N^2+p_\perp^2}{p_f^+p_i^+}q^+. \tag{B12}$$

The scalar products of initial ($p^{\mu}_{i,\mathrm{on}}$), final (p^{μ}_{f}), and transferred (q^{μ}) momenta with the off-shell factor Δp^{μ}_{i}, can be written as:

$$
\begin{aligned}
2\Delta p_i \cdot p_i &= Q^2 \frac{\alpha_N}{\alpha_q} - \left(m_N^2 + \mathbf{p_T}^2\right)\frac{\alpha_q}{\alpha_f} \\
2\Delta p_i \cdot p_f &= Q^2 \frac{\alpha_f}{\alpha_q} - \left(m_N^2 + \mathbf{p_T}^2\right)\frac{\alpha_q}{\alpha_i} \\
2\Delta p_i \cdot q &= Q^2 - \left(m_N^2 + \mathbf{p_T}^2\right)\frac{\alpha_q^2}{\alpha_f \alpha_N}.
\end{aligned}
\tag{B13}
$$

[1] N. Fomin, D. Higinbotham, M. Sargsian, and P. Solvignon, Annu. Rev. Nucl. Part. Sci. **67**, 129 (2017).
[2] O. Hen, G. A. Miller, E. Piasetzky, and L. B. Weinstein, Rev. Mod. Phys. **89**, 045002 (2017).
[3] W. Boeglin and M. Sargsian, Int. J. Mod. Phys. E **24**, 1530003 (2015).
[4] C. Ciofi degli Atti, Phys. Rep. **590**, 1 (2015).
[5] J. Arrington, D. W. Higinbotham, G. Rosner, and M. Sargsian, Prog. Part. Nucl. Phys. **67**, 898 (2012).
[6] L. Frankfurt, M. Sargsian, and M. Strikman, Int. J. Mod. Phys. A **23**, 2991 (2008).
[7] L. L. Frankfurt, M. I. Strikman, D. B. Day, and M. Sargsian, Phys. Rev. C **48**, 2451 (1993).
[8] K. S. Egiyan *et al.* (CLAS Collaboration), Phys. Rev. C **68**, 014313 (2003).
[9] K. S. Egiyan *et al.* (CLAS Collaboration), Phys. Rev. Lett. **96**, 082501 (2006).
[10] N. Fomin *et al.*, Phys. Rev. Lett. **108**, 092502 (2012).
[11] A. Tang, J. W. Watson, J. Aclander, J. Alster, G. Asryan, Y. Averichev, D. Barton, V. Baturin, N. Bukhtoyarova, A. Carroll, S. Gushue, S. Heppelmann, A. Leksanov, Y. Makdisi, A. Malki, E. Minina, I. Navon, H. Nicholson, A. Ogawa, Y. Panebratsev, E. Piasetzky, A. Schetkovsky, S. Shimanskiy, and D. Zhalov, Phys. Rev. Lett. **90**, 042301 (2003).
[12] R. Shneor *et al.* (Jefferson Lab Hall A Collaboration), Phys. Rev. Lett. **99**, 072501 (2007).
[13] E. Piasetzky, M. Sargsian, L. Frankfurt, M. Strikman, and J. W. Watson, Phys. Rev. Lett. **97**, 162504 (2006).
[14] R. Subedi *et al.*, Science **320**, 1476 (2008).
[15] M. M. Sargsian, Phys. Rev. C **89**, 034305 (2014).
[16] O. Hen *et al.*, Science **346**, 614 (2014).
[17] O. Artiles and M. M. Sargsian, Phys. Rev. C **94**, 064318.
[18] L. L. Frankfurt, M. M. Sargsian, and M. I. Strikman, Phys. Rev. C **56**, 1124 (1997).
[19] M. M. Sargsian, Int. J. Mod. Phys. E **10**, 405 (2001).
[20] C. Ciofi degli Atti and L. P. Kaptari, Phys. Rev. C **71**, 024005 (2005).
[21] S. Jeschonnek and J. W. Van Orden, Phys. Rev. C **78**, 014007 (2008).
[22] J. M. Laget, Phys. Lett. B **609**, 49 (2005).
[23] M. M. Sargsian, T. V. Abrahamyan, M. I. Strikman, and L. L. Frankfurt, Phys. Rev. C **71**, 044614 (2005).
[24] M. M. Sargsian, T. V. Abrahamyan, M. I. Strikman, and L. L. Frankfurt, Phys. Rev. C **71**, 044615 (2005).
[25] M. M. Sargsian, Phys. Rev. C **82**, 014612 (2010).
[26] W. Cosyn and M. Sargsian, Phys. Rev. C **84**, 014601 (2011).
[27] W. Cosyn and M. Sargsian, Int. J. Mod. Phys. E **26**, 1730004 (2017).
[28] A. Bussiere *et al.*, Nucl. Phys. A **365**, 349 (1981).
[29] S. Turck-Chieze *et al.*, Phys. Lett. B **142**, 145 (1984).
[30] J. F. J. van den Brand, H. P. Blok, R. Ent, E. Jans, G. J. Kramer, J. B. J. M. Lanen, L. Lapikas, E. N. M. Quint, G. van der Steenhoven, and P. K. A. deWitt Huberts, Phys. Rev. Lett. **60**, 2006 (1988).
[31] S. Frullani and J. Mougey, Adv. Nucl. Phys. **14**, 1 (1984).
[32] T. de Forest, Nucl. Phys. A **392**, 232 (1983)
[33] R. P. Feynman, *Photon-Hadron Interactions* (Westview Press, Reading, 1972).
[34] J. Kogut and D. Soper, Phys. Rev. D **1**, 2901 (1970).
[35] G. P. Lepage and S. J. Brodsky, Phys. Rev. D **22**, 2157 (1980).
[36] L. L. Frankfurt and M. I. Strikman, Phys. Rep. **76**, 215 (1981).
[37] S. J. Brodsky, H. C. Pauli, and S. S. Pinsky, Phys. Rep. **301**, 299 (1998).
[38] L. L. Frankfurt and M. I. Strikman, Nucl. Phys. B **148**, 107 (1979).
[39] B. D. Keister and W. N. Polyzou, Adv. Nucl. Phys. **20**, 225 (1991).
[40] G. A. Miller, Prog. Part. Nucl. Phys. **45**, 83 (2000).
[41] W. W. Buck and F. Gross, Phys. Rev. D **20**, 2361 (1979).
[42] S. D. Glazek, Acta Phys. Polon. B **14**, 893 (1983).
[43] G. A. Miller, Phys. Rev. C **89**, 045203 (2014).
[44] A. M. Bincer, Phys. Rev. **118**, 855 (1960).
[45] H. W. L. Naus, S. J. Pollock, J. H. Koch, and U. Oelfke, Nucl. Phys. A **509**, 717 (1990)
[46] S. J. Pollock, H. W. L. Naus, and J. H. Koch, Phys. Rev. C **53**, 2304 (1996)
[47] J. J. Aubert *et al.* (European Muon Collaboration), Phys. Lett. B **123**, 275 (1983).
[48] W. U. Boeglin *et al.*, arXiv:1410.6770 [nucl-ex].